buildings

MDPI

Article

Leakage Diagnosis of Air Conditioning Water System Networks Based on an Improved BP Neural Network Algorithm

Rundong Liu [1,2,3,*], Yuhang Zhang [4] and Zhengwei Li [4]

[1] School of Environmental Science and Engineering, Suzhou University of Science and Technology, Suzhou 215009, China
[2] Jiangsu Province Key Laboratory of Intelligent Building Energy Efficiency, Suzhou University of Science and Technology, Suzhou 215009, China
[3] National and Local Joint Engineering Laboratory of Municipal Sewage Resource Utilization Technology, Suzhou 215009, China
[4] School of Mechanical and Energy Engineering, Tongji University, Shanghai 200092, China; 1932711@tongji.edu.cn (Y.Z.); zhengwei_li@tongji.edu.cn (Z.L.)
* Correspondence: lrd@mail.usts.edu.cn

Abstract: Compared with traditional pipe networks, the complexity of air conditioning water systems (ACWSs) and the alternation of cooling and heating are more likely to cause pipe network leakage. Pipe leakage failure seriously affects the reliability of the air conditioning system, and can cause energy waste or reduce human comfort. In this study, a two-stage leakage fault diagnosis (LFD) method based on an Adam optimization BP neural network algorithm, which locates leakage faults based on the change values of monitoring data from flow meters and pressure sensors in air conditioning water systems, is proposed. In the proposed LFD method, firstly, the ACWS network's hydraulic model is built on the Dymola platform. At the same time, a cuckoo algorithm is used to identify the pipe network's characteristics to modify the model, and the experimental results show that the relative error between the model-simulated value and the actual values is no more than 1.5%. Secondly, all possible leakage conditions in the network are simulated by the model, and the dataset is formed according to the change rate of the observed data, and is then used to train the LFD model. The proposed LFD method is verified in a practical project, where the average accuracy of the first-stage LFD model in locating the leaking pipe is 86.96%; The average R^2 of the second-stage LFD model is 0.9028, and the average error between the predicted location and its exact location with the second-stage LFD model is 6.3% of the total length of the leaking pipe. The results show that the proposed method provides a feasible and convenient solution for timely and accurate detection of pipe network leakage faults in air conditioning water systems.

Keywords: BP neural network; air conditioning water systems; leakage fault diagnosis

Citation: Liu, R.; Zhang, Y.; Li, Z. Leakage Diagnosis of Air Conditioning Water System Networks Based on an Improved BP Neural Network Algorithm. *Buildings* **2022**, *12*, 610. https://doi.org/10.3390/buildings12050610

Academic Editors: Shi-Jie Cao, Dahai Qi, Junqi Wang and Gwanggil Jeon

Received: 31 March 2022
Accepted: 5 May 2022
Published: 6 May 2022

1. Introduction

With people's aspirations and pursuit of a better life, the requirements for indoor air quality have gradually increased [1], and centralized or semi-centralized central air conditioning systems are being more and more widely used in today's buildings. As an important part of air conditioning systems, the pipe network not only plays an important role in connecting the unit, the air conditioning terminal device, and the cooling side, but also undertakes the key task of transporting and distributing the cold or heat to each terminal device. However, as the use of air conditioning systems grows over the years, many factors—such as the pipe material, surrounding environment, laying method,

construction quality, and operation and maintenance management—affect the reliability of the air conditioning water system (ACWS) pipe network, and pipe leakage has become one of the most frequent failures in the whole life cycle of air conditioning systems [2].

Usually, ACWSs are equipped with water make-up devices, so a small leakage in the pipe network is often not obvious, and is often overlooked. However, pipe leakage failure often causes immeasurable damage to the actual running of the system. Figure 1 shows the common forms of damage to ACWS pipe networks. The "Practical Heating and Air Conditioning Design Manual" [3] stipulates the hourly leakage and replenishment of the ACWS. If a large public building is designed according to this standard with a floor area of 20,000 m^2, the hourly make-up water to the ACWS due to pipe network leakage is 800 L. At the same time, the make-up water is cold or hot water treated by high-priced softening; in addition to the large waste of water resources and energy consumption, pipe network leakage may also cause the system to deviate from the best working operating point [4], thus affecting human comfort. Pipe network leakage has become the most common but difficult-to-deal-with problem in ACWS failures. In addition, the vast majority of accidents in the pipe network do not occur suddenly, but are gradual, slow processes [5]. Pipe network leakage is a precursor to major accidents, such as long-term neglect of the leakage problem which, in the event of an accident, can seriously threaten people's lives and the safety of their property. Therefore, if the pipe leakage can be detected and solved in a timely manner, one can not only avoid the waste of water resources and energy consumption by the system, but also prevent the problem before it occurs, effectively reducing the possibility of safety accidents such as pipe bursts.

(**a**) (**b**)

Figure 1. Common forms of damage to ACWS pipe networks: (**a**) leakage causes ACWS performance degradation; (**b**) ACWS water leakage causes mildew.

The key means of solving leakage problems in pipe networks is to use scientific and effective pipe network leakage detection methods to accurately locate the location of the leak(s) in the faulty pipe network. Discussion has been made of various pipeline fault detection methods, viz., vibration analysis, pulse-echo methodology, acoustic techniques, negative-pressure-wave-based leak detection systems, support-vector machine (SVM)-based pipeline leakage detection, interferometric-fiber-sensor-based leak detection, filter diagonalization method (FDM), etc. It was found that these methods have been applied for specific fluids, such as oil, gas, and water [6]. In air conditioning systems, the popularity of temperature, pressure, and flow sensors has led many scholars to propose diagnostic methods for pipe leakage based on statistical or analytical methods, including the pressure gradient method [7], pressure point analysis [8], negative pressure wave method [9], and extended Kalman filter [10] (the leakage position is determined using the 9-DOF IMU (3D accelerometer, 3D gyroscope, and 3D magnetometer) sensor data in the extended Kalman filter), which were found to have

limited application scenarios based on examples, or to be more appropriate as auxiliary diagnostic tools.

With the development of artificial neural network technology, more and more scholars are exploring the possibilities of this technology for identifying pipe network leakage faults [11–13]. Lei et al. [14] established a BP-neural-network-based heating pipe network leakage fault diagnosis model based on artificial neural network, and introduced the idea of hierarchy into pipe network leakage diagnosis. Duan et al. [15] established an adaptive neuro-fuzzy inference system (ANFIS)-based LFD model for centralized heating pipe networks. The example verified that the ANFIS-based heat network LFD model is stable and has high diagnostic accuracy. Xue et al. [16] proposed an XGBoost-based district heating network leakage diagnosis method, using the rate of change of observed data from the flow and pressure sensors installed in the system to locate the leaky pipe section. A series of studies have shown that the technology applied to district heating networks (DHNs) has good diagnostic accuracy and stability—especially BP neural networks, which show a strong ability of nonlinear fitting and self-sample learning. However, with the increasing volume and complexity of ACWS networks, the traditional manual inspection or hardware-based network leakage diagnosis methods struggle to meet the requirements of "quick, accurate and steady" diagnosis of leakage faults in ACWS networks [14].

While there are a few studies on ACWS leakage diagnosis, this study focuses on the actual diagnosis effect of a BP neural network algorithm on the ACWS leakage problem. In addition, most of the pipe network LFD methods mentioned above regard the leaking pipe's number as the final diagnosis result. When the leaking pipe is long, this causes problems with the diagnostic efficiency. Leakage diagnosis of pipelines can prevent environmental and financial losses [17], and instability of air conditioning water systems can lead to lower energy efficiency of air conditioning systems [18]. This study aims to diagnose pipes' exact leakage location after diagnosing the identity of the leaking pipe. Compared with DHNs, ACWSs are more directly customer-facing, and affect the customer experience more quickly when they leak. Therefore, compared with other networks, it is more necessary to study the leakage diagnosis of ACWS networks, and to explore the feasibility of BP neural network technology for practical applications.

This paper proposes the possibility of applying an Adam-optimized BP neural network algorithm to the diagnosis of pipe leakage in ACWSs, establishes a simulated hydraulic model of pipe network leakage based on the Dymola platform (a kind of engineering modeling platform, detailed in Section 2.2.1), adopts the cuckoo search algorithm to identify the characteristics of the pipe network so as to ensure the reliability and accuracy of the simulation model, proposes a two-stage leakage diagnosis method with the Adam-optimized BP neural network—which not only locates the leaky pipe section, but also locates the exact leakage point on the pipe—and demonstrates the application of the method based on a practical project.

The rest of this paper is organized as follows: Section 2 briefly describes the research methodology, with practical examples. Section 3 shows and analyzes the actual results of the method. Section 4 discusses the case results and implications. Section 5 presents the main conclusions of this study.

2. Materials and Methods

2.1. Research Overview

Figure 2 shows the research path and design ideas of this paper, and the methods used are detailed in the subsequent section.

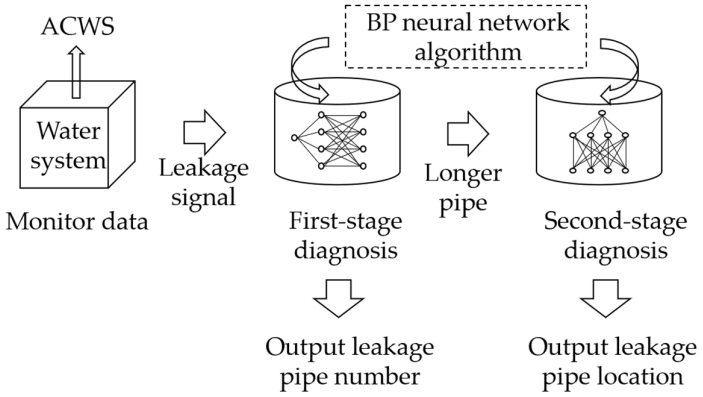

Figure 2. Research path and design ideas.

Figure 3 shows the detailed diagnosis process. When the ACWS is stable, the leakage diagnosis is triggered by monitoring the make-up water's flow rate (if the pipe network system is not installed with a make-up water flow sensor, the difference between the water supply's main flow rate and the return's main flow rate is used as the make-up water flow rate) when the set threshold is exceeded in the duration (which can be set). The real-time data (i.e., flow rate and pressure) monitored by the system are provided to the pipe network model and the BP neural network for second-stage diagnosis, respectively, and the first-stage diagnosis is performed by the sample set of leak conditions from the Dymola pipe network water system model, which outputs the identification number of its leaky pipe section. At the same time, to determine whether the length of the pipe section exceeds the set threshold length, if the length of the pipe section is shorter than the set threshold, the second-stage diagnosis is skipped and the network fault information is output directly; if the length of the pipe section is longer than the set threshold, the second-stage diagnosis is triggered, and the exact location of the leakage and the identity of the leaky pipe section are output as the results of the fault information to complete the accurate identification of the leakage fault in the ACWS.

The ACWS network hydraulic model was built on the Dymola platform (detailed in Section 2.2.1); the identification of network resistance characteristics by the cuckoo algorithm (detailed in Section 2.2.2) helps to improve the hydraulic model and ensure that the model is as close as possible to the actual system. Meanwhile, the two-stage leakage diagnosis methods of the pipe network were all built using an Adam-optimized BP neural network, with different parameters set according to the different output variables of the two stages (detailed in Section 2.2.3).

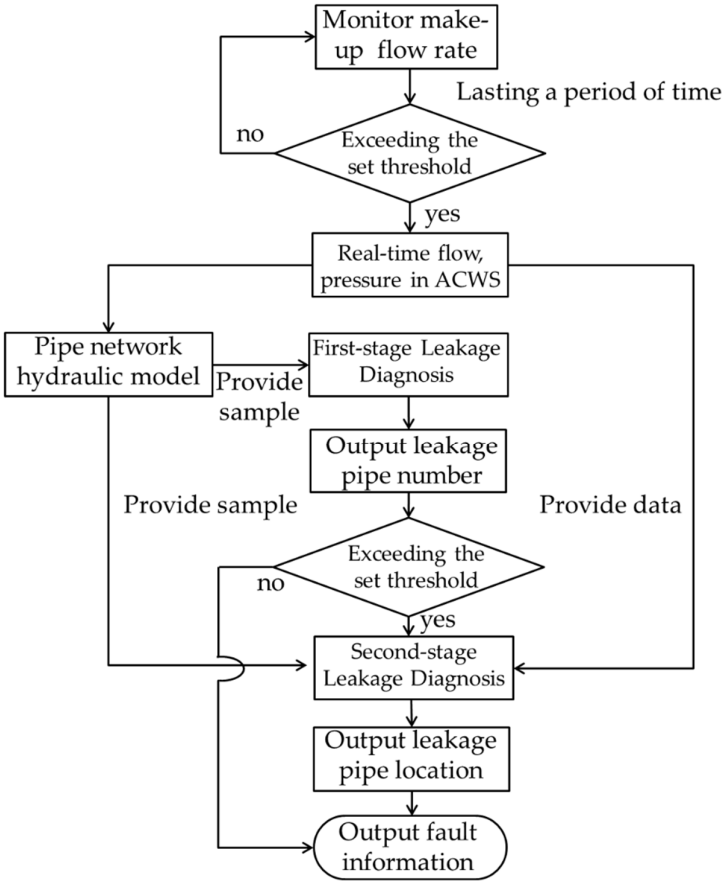

Figure 3. Research diagram of two-stage leakage diagnosis in ACWSs.

2.2. Method Description

2.2.1. Hydraulic Model of the ACWS Network under Simulated Leakage Conditions

The Dymola platform is a multidisciplinary system modeling and simulation tool based on the Modelica language (an object-oriented physical modeling language) [19]. It has a library of models and simulation specialties suitable for multiple engineering domains, and has proven its applicability in the engineering field, while "Modelica.Fluid" provides the basis for developing the network hydraulic model. However, the existing components cannot meet the simulation under leakage conditions, so for this paper we developed a hydraulic model that can simulate different leakage conditions based on the Dymola platform.

The model is shown in Figure 4. In the event that a leak occurs at a certain point on the pipe, the simulated leakage is divided into two pipes—"pipe1" and "pipe2"—and the two pipes are connected by a tee junction without pressure loss, and then connected by a "negative flow source" (corresponding to the source module in Figure 4), which can be set by the user. All of the above components are "packaged" into a new element.

By setting the flow rate of the "negative flow source" and the ratio of the length of each pipe to the total pipe length (i.e., the simulated pipe leakage volume and leakage location), the model is built under different leakage conditions. In order to verify the accuracy of the hydraulic model of the pipe leakage, the classical theoretical calculation method and the simulation method based on the hydraulic model are used to calculate the pressure difference between the inlet and outlet of the same pipe, and the model is verified by comparing the calculation results (details in Appendix A).

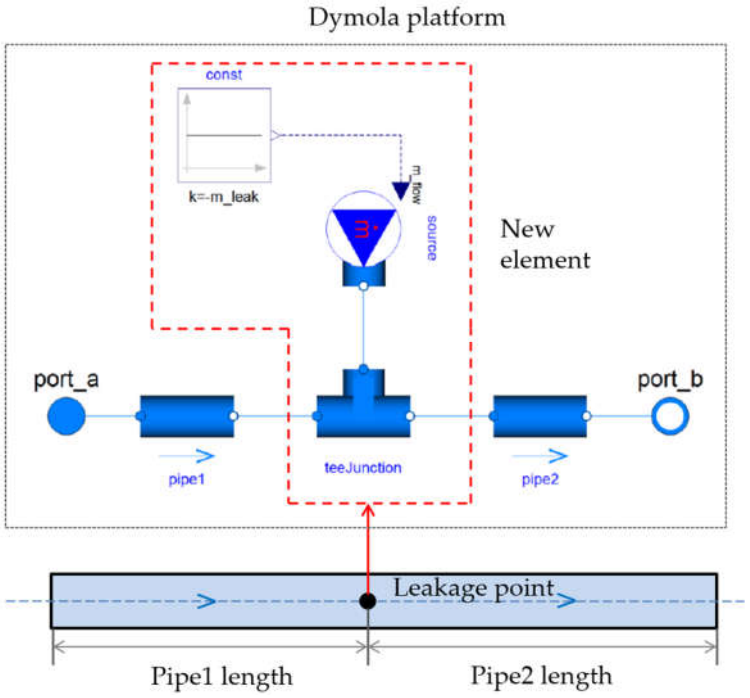

Figure 4. Hydraulic model of pipe leakage on the Dymola platform.

2.2.2. Cuckoo Search Algorithm for the Identification of Network Resistance Characteristics

The hydraulic model established using Dymola described in Section 2.2.1 is not sufficient to simulate the actual pipe network system. In the actual pipe network, there are factors such as pipe corrosion, internal wall scaling, etc. The resistance characteristics of the pipe network inevitably deviate from the initial design calculation values, and the key to establishing an accurate hydraulic model of the pipe network lies in the identification of the resistance characteristics of the pipe network. Optimization algorithms are a common method for the identification of pipe network resistance characteristics. The performance of the cuckoo search algorithm was compared with that of the particle swarm algorithm, differential evolution algorithm, artificial bee swarm algorithm, and other algorithms based on various test functions [20], showing that the cuckoo search algorithm has fewer parameters, simple operation, easy implementation, generality and robustness, and excellent local and global search capabilities with comprehensive advantages. Meanwhile, the object of this paper is similar to the research objects in the literature on the identification of pipe resistance characteristics, so the cuckoo search algorithm was used in this study to help improve the hydraulic model.

Before applying the optimization algorithm, it is necessary to determine the objective function of the identification of the resistance characteristics of the pipe network in this study. The purpose is that the final identification parameters optimized by the algorithm can make the simulated parameters of the hydraulic model as close as possible to the actual monitored values. In this study, the sum of the absolute value of the relative error between the actual monitored values and the model-simulated values of each sensor (pressure and flow rate) in the pipe network system is used as the objective function, and the formula is shown in Equation (1):

$$obj(S) = \sum_{z=1}^{Z}\left(\sum_{i=1}^{N_P}\left|\frac{P_s - P_m}{P_m}\right| + \sum_{j=1}^{N_Q}\left|\frac{Q_s - Q_m}{Q_m}\right|\right) \quad (1)$$

where Z is the number of conditions involved in the calibration; N_P and N_Q represent the numbers of pressure and flow sensors installed in the network system, respectively; P_m,

and P_s represent the monitored and simulated pressures, respectively; and Q_m and Q_s represent the monitored and simulated pipe section flow rates, respectively. There are also implicit constraints between the simulated pressure P_s and the simulated pipe flow Q_s, i.e., the hydraulic balance equations (i.e., nodal continuity equation, basic loop energy equation, and Bernoulli's equation) of the network itself need to be met.

The process of identifying the resistance characteristics of the ACWS network based on the cuckoo search algorithm is as follows:

Step 1: Build a pipe network simulation model based on deterministic parameters.

Step 2: Set parameters such as population size, discovery probability P_a, maximum number of iterations N of the algorithm, and random initialization of bird's nest locations, with each set of bird's nest locations representing a set of pipe resistance characteristic coefficients to be identified.

Step 3: Substitute each nesting position into the pipe network simulation model to calculate the objective function value of each nesting position (i.e., each set of pipe resistance characteristic coefficients), and compare them to obtain the current optimal nesting position and the optimal objective function value.

Step 4: Keep the optimal nest location in the previous generation, update the nest locations other than the optimal nest using Lévy flight, and calculate the corresponding objective function value, compare the obtained objective function value with the current optimal value, and update the current optimal objective function value [21].

Step 5: Compare the random number r with the discovery probability P_a. If $r > P_a$, change the nest location once randomly; if not, keep it the same. Finally, retain the optimal set of nest locations.

Step 6: If the maximum number of iteration generations has been reached or the search precision requirement has been met, continue to the next step; otherwise, return to Step 4

Step 7: Output the global optimal nest location, which is the optimal resistance coefficient of the pipe network in this search process.

The optimal results obtained according to the above steps are used as the pipe network resistance coefficients of the hydraulic model, making the hydraulic model more accurate and closer to the actual operation of the system.

2.2.3. Adam Optimization Algorithm for the LFD Model

"BP neural network" usually refers to multilayer feedforward neural networks trained with the error backpropagation (BP) algorithm. BP neural networks have been widely used in many engineering fields—such as pattern recognition, intelligent control, fault diagnosis, image recognition processing, and optimization computation—due to their nonlinear mapping capability, self-learning and self-adaptive capability, and generalization capability.

The Adam (adaptive moment estimation) optimization algorithm is an improved algorithm for traditional BP neural networks, which adopts independent adaptive learning rates for different parameters by calculating the first-order moment estimation and second-order moment estimation of the gradient during the training of the neural network [22]. It has been experimentally shown that neural networks based on the Adam optimization algorithm not only have faster training speed compared to other stochastic optimization methods, but also do not easily fall into local optima, and have excellent performance in practice. Therefore, this study uses the Adam optimization algorithm as the kernel for the LFD model of the ACWS.

This paper adopts the concept of hierarchy in the structure of the LFD model [23]. On the one hand, the ACWS undertakes the building's heat and cold load, and there are a variety of control methods, such as fixed-flow and variable-flow systems, variable-flow systems that contain the supply and return main-fixed temperature control systems, supply and return main-fixed differential pressure control systems, and the most unfavorable end-fixed differential pressure control systems. The control system is

complex; on the other hand, the length of each pipe section in the ACWS is unevenly distributed, and the number of stages varies greatly—the long pipes may be hundreds of meters, while the short pipes may only be one or two meters. If all the pipes are diagnosed with leakage faults, this will affect the diagnosis time and reduce efficiency, while there is research showing that two-stage fault diagnosis, compared to single-fault diagnosis (a single diagnosis to identify the section of the leaky pipe and the leakage location), has higher diagnostic accuracy as well as relatively less training time [24], which not only reduces the complexity of fault diagnosis and the training time of diagnosis, but can also adjust the fault diagnosis process and improve the efficiency of fault diagnosis according to the user's needs in the actual application process. Therefore, this paper uses the two-stage LFD model for fault diagnosis of the ACWS pipe network.

The leakage conditions are simulated by the improved hydraulic model, and the sample datasets under different conditions are obtained. Then, the two-stage LFD model is trained by setting the parameters of the Adam optimization algorithm (such as the number of hidden layer nodes, the activation function of the hidden layer, and the regularization parameter). The training and testing process of the neural network was achieved in this study using the Python programming language.

2.2.4. LFD Model Performance Evaluation Indicators

In order to verify the application effect of the LFD model, it is also necessary to introduce indicators to measure the performance of the two-stage LFD model [25]. Since the two-stage LFD models solve different types of problems, different performance evaluation indicators need to be used, as shown in Table 1.

First-stage diagnosis is a typical multiple-classification task, so it uses the model performance evaluation indicators commonly used for classification tasks: precision, recall, and F_1 score. For the binary classification task, the samples can be classified into four cases according to the combination of true and predicted categories: *TP* (true positive), *FP* (false positive), *TN* (true negative), and *FN* (false negative).

Second-stage diagnosis is a typical regression task, so its performance needs to be evaluated using different evaluation indicators from first-stage leakage diagnosis. The commonly used performance evaluation indicators for regression tasks are shown in Table 1, where m denotes the total number of samples, y_i represents the true marker of x_i, $\hat{y}_i$ represents the prediction result of the learner for x_i, and $\overline{y}_i$ represents the average of the m sets of true values.

Table 1. Model performance evaluation indicators.

	Performance Evaluation Indicators	Definitions
First-stage diagnosis model	$Accuracy$	$Accuracy = \frac{TP + TN}{TP + TN + FP + FN}$
	P	$P = \frac{TP}{TP + FP}$
	R	$R = \frac{TP}{TP + FN}$
	F_1	$F_1 = \frac{2PR}{P + R}$
Second-stage diagnosis model	MSE (mean squared error)	$MSE = \frac{1}{m}\sum_{i=1}^{m}(y_i - \hat{y}_i)^2$
	MAE (mean absolute error)	$MAE = \frac{1}{m}\sum_{i=1}^{m}\lvert y_i - \hat{y}_i \rvert$
	R^2 (coefficient of determination)	$R^2 = 1 - \frac{\sum_{i=1}^{m}(\hat{y}_i - y_i)^2}{\sum_{i=1}^{m}(\overline{y}_i - y_i)^2}$

2.3. Case Study

Taking a Guangzhou (China) metro station's ACWS system pipe network project as an example, the ACWS form is a primary pump variable-flow system with fixed differential pressure control for the supply and return mains. The chilled water system has a supply and return water temperature of 10 and 17 °C, respectively. The system pressure point is set at the entrance of the circulating water pump, and the pressure is 32.3 kPa. Pressure sensors are set for the cold source and each terminal device's import and export, and flow sensors are set for the chilled water main pipe and each terminal device's return branch pipe.

In order to model the actual pipe network system on the Dymola platform, the system needs to be reasonably simplified, as follows: ① the chiller, the pump, and other equipment in the room are combined into one node (cold source); ② if two pipes are connected and there is no node in the middle, the two pipes are combined into the same pipe; ③ the local resistance of the fittings in the pipe is expressed using the length of the straight pipe section of the same diameter as the connected pipe (i.e., the local resistance's equivalent length). The supply and return water system, with pipe section numbers, is shown in Figure 5.

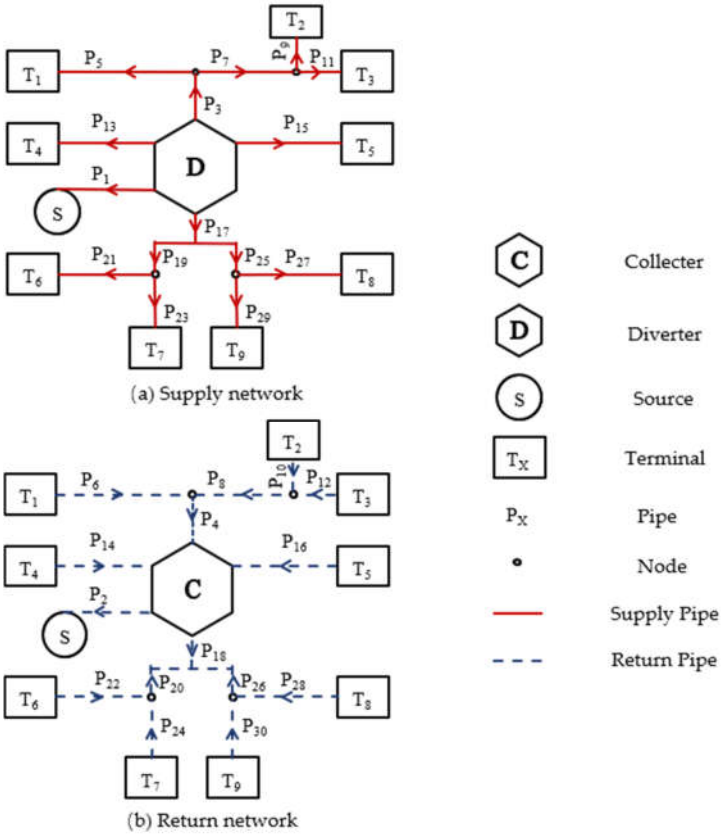

Figure 5. Supply and return of water in the ACWS network.

The case pipe network includes 1 cold source (S), 9 terminal devices (T1–T9), 30 pipes (pipe1–pipe30), and 31 sensor monitoring points (11 flow sensors and 20 pressure sensors), where the basic parameters of each pipe section are shown in Figure 6.

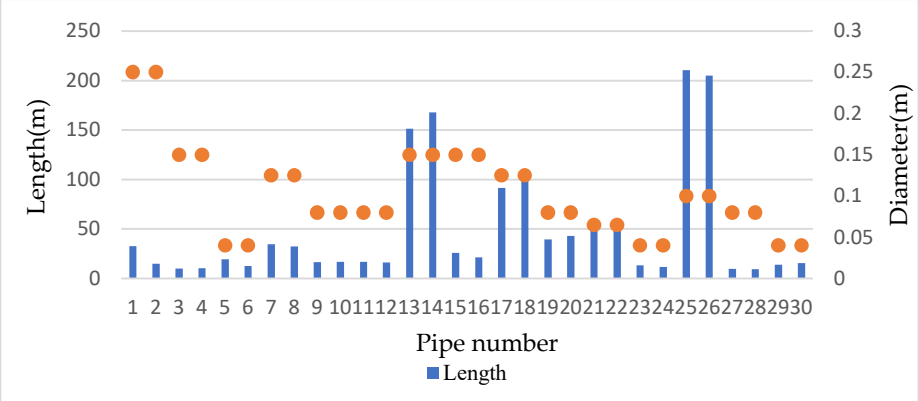

Figure 6. Basic parameters of the case pipe network.

The cuckoo search algorithm was used to identify the resistance characteristics of the case pipe network, and the parameters are shown in Table 2. The training curves of the optimization algorithms show that when the number of iterations reaches 100, the average and optimal fitness values of the algorithms no longer decrease significantly, and the algorithms can be considered to have reached convergence. In order to avoid the random error in the single identification process, the algorithm was operated independently 10 times, and the average value of the 10 identification results was taken as the final result of the identification of the resistance characteristics of the pipe network.

Table 2. Parameter settings of the cuckoo search algorithm used for the identification of resistance characteristics.

Parameter	Setting
Population size of each generation	50
Discovery probability	0.25
Maximum number of iterations	100

A sufficient number of training samples is a prerequisite for a satisfactory diagnostic performance of a pipe network LFD model, and the more comprehensive the leakage conditions contained, the more abundant the training data, and the better the performance of the final training diagnostic model. However, it is very difficult—almost impossible—to obtain a large and comprehensive set of fault condition data via experimental testing or historical data logging for the ACWS network in this case. Therefore, the Dymola model simulation was used to obtain the data samples required for the training of the LFD model. The simulated leakage conditions were as follows: for each pipe leak point setting in the case study, the ratio of the distance from the start of the pipe section to the total pipe length was selected as 0.05, 0.1, 0.15, 0.2, 0.25, 0.3, 0.35, 0.4, 0.45, 0.5, 0.55, 0.6, 0.65, 0.7, 0.75, 0.8, 0.85, 0.9, or 0.95, while the ratio of the possible leakage volume from the total circulating water volume was selected as 1%, 1.5%, 2%, 2.5%, 3%, 3.5%, 4%, 4.5%, or 5%.

According to the above setting conditions, for the 30 pipes in the case pipe network system, each pipe has 19 possible leakage points, and each leakage point can have 9 different degrees of leakage. For each leakage working condition, 5130 sets of simulated data samples can be obtained, one by one. At the same time, taking into account the random error of the sensor measurement process in the actual case, a certain amount of artificial noise is added to the original data generated by the simulation model, and the artificially added noise X follows a normal distribution with a mean of 0 and a standard deviation of σ. The accuracy level of the case pipe network sensor is 0.2%FS (full-scale,

range), and according to the "3σ" criterion of normal distribution, σ is taken as 1/3 of 0.2% FS.

In the settings of the first-stage LFD model, all data samples are randomly divided into a training set and a test set at a ratio of 9:1. The random partitioning process takes the form of stratified sampling. The training set is used to train the BP neural network model, while the test set is used to replace the fault data monitored in the actual case. The neural network adopts a single-hidden-layer structure. The parameter settings of the Adam optimization BP neural network algorithm used for the first-stage LFD model are presented in Table 3.

Table 3. Parameter settings of the Adam optimization BP neural network algorithm used for the first-stage LFD model.

Parameter	Setting
Number of hidden layer nodes	31
Activation function of hidden layer	Identity function
Regularization parameter	0.0001
Maximum number of iterations	3000
Convergence precision	1×10^{-4}

In the settings of the second-stage LFD model, the length threshold θ_L = 50 m is set as the basis for determining whether to perform secondary diagnosis of leaks according to the conditions of the case system. The output of the second-stage LFD model is the exact location of the leakage point in the ACWS, which is expressed as the distance of the leakage point from the beginning of the pipe section/the total length of the leakage pipe. Due to the fact that the second-stage LFD model is also based on the BP neural network model, its training and testing methods are essentially the same as those of the first-stage LFD model. Some of the settings are different, as follows: the training and testing sets are randomly divided at a ratio of 7:3, and the activation function is a ReLU function.

3. Results

3.1. Results of Identification of the Case Pipe Network's Characteristics

The flow and pressure parameters of four groups of case pipe networks under regular conditions were selected as the original data for solving the objective function of pipe network resistance characteristic identification, and another set of flow and pressure data were selected to verify the effect of identification of the pipe network resistance characteristics based on the cuckoo search algorithm. In order to avoid the accidental error of the single identification process, the algorithm was operated 10 times independently, and the average value was taken as the final result, as shown in Table 4.

Table 4. Results of identification of the case pipe network's characteristics.

Pipe Number	Coefficient of Pipe Resistance Characteristic (s^2/m^5)	Pipe Number	Coefficient of Pipe Resistance Characteristic (s^2/m^5)
1	53.3	16	588.0
2	24.0	17	6188.9
3	267.4	18	6749.5
4	277.5	19	32,186.2
5	487,138.3	20	32,118.5
6	344,413.0	21	119,729.4
7	2257.2	22	115,777.9
8	2249.1	23	426,030.6
9	11,666.6	24	383,965.0

10	11,909.8	25	52,034.0
11	12,438.9	26	43,475.3
12	12,068.8	27	7121.1
13	4295.8	28	7064.7
14	4421.0	29	347,589.0
15	718.9	30	414,020.7

As shown in Table 4, from the identification results of the pipe network's resistance characteristics, we found that the resistance characteristic coefficient of each pipe section was quite different; the smallest was 24 s^2/m^5, and the largest was 487,138.3 s^2/m^5. The main reason for this was the large difference in the pipes' length in the case system, and the internal situation of the pipe network was also different.

Due to the fact that the actual monitored values of the pipe network contain only two parameters of flow and pressure, it was necessary to substitute the results of the optimal pipe network resistance characteristic coefficients identified by the algorithm into the hydraulic model of the pipe network, and to evaluate the identification accuracy and precision of the algorithm by comparing the simulated values with the actual monitored values of flow and inlet/outlet pressure at each terminal, the results of which are shown in Figure 7.

It was found that the optimal identification of the pipe resistance characteristic coefficients based on the cuckoo algorithm was largely consistent with the actual monitored values after being substituted into the original hydraulic model. As depicted in Figure 7a, the minimum difference in flow rate was 0.04 m^3/h, while the maximum difference was 0.63 m^3/h. As depicted in Figure 7b, the minimum difference in pressure was 0.02 kP_a, and the maximum difference was 0.3 kP_a. Further discussing the identification results of the pipe network's resistance characteristics, it can be observed that the average relative error between the monitored and simulated values of the flow rate at each terminal was 1.358%, the average relative error between the monitored and simulated values of the water supply pressure at each terminal was 0.057%, and the average relative error between the monitored and simulated values of the return water pressure at each terminal was 0.089%.

The above data show that the hydraulic model optimized by the cuckoo search algorithm to identify the resistance characteristics achieves an acceptable error range for the actual project. This verifies that this method can be used for the calibration and optimization of the ACWS hydraulic model, and also provides technical possibilities for application in other complex pipe networks, such as heating and municipal pipe networks. Due to the leakage condition dataset used to train the two-stage LFD model being generated from the hydraulic model simulation, the hydraulic model has a significant impact on the LFD model simulation results.

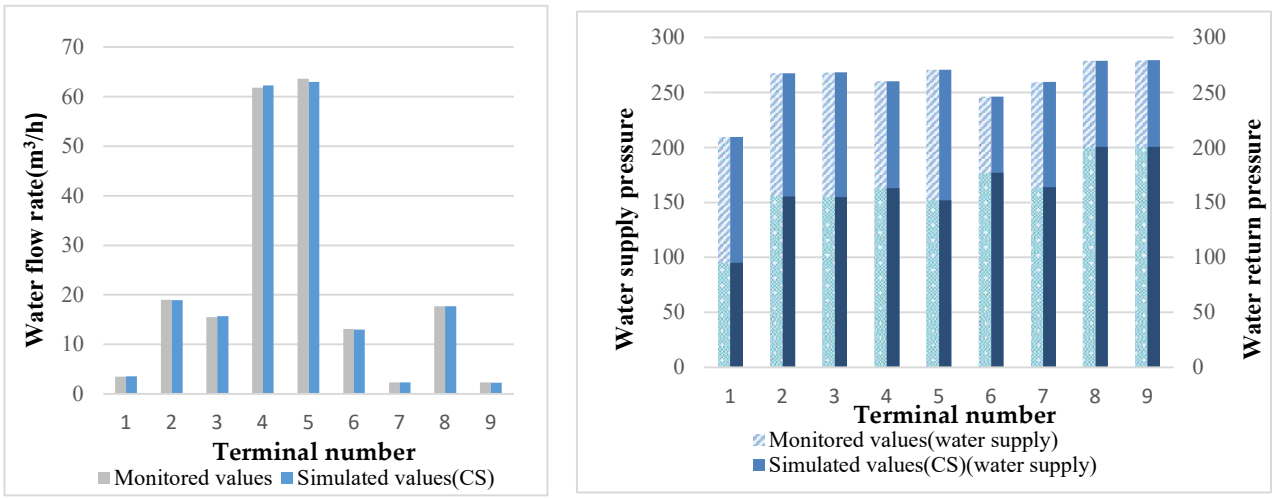

(**a**) (**b**)

Figure 7. (**a**) Comparison of monitored and simulated flow values. (**b**) Comparison of monitored and simulated pressure values.

3.2. Results of the First-Stage LFD Model

Before testing the model, it is necessary to set the neural network's number of hidden layer nodes, because the number of nodes affects the performance of the LFD model. It has been shown in the literature [26] that if the number of hidden layer nodes is too small, the neural network will lack the necessary learning ability and information processing ability. If the number of hidden layer nodes is too large, it will not only greatly increase the complexity of the neural network structure, and make the neural network more likely to fall into local minima during the learning process, but also make the learning speed of the neural network very slow. The range of node numbers is determined with a commonly used empirical formula, and then tested and adjusted to obtain the optimal number of hidden layer nodes for the neural network.

According to the settings of the first-stage LFD model (detailed parameter settings are shown in Table 3), we used the Python programming language for the training and testing of the neural network. A total of 100 experiments were repeated to avoid the random error caused by a single experiment. Each time, the dataset was resampled to obtain a new training set and test set, and the average of 100 experiments was taken as the final result of the first-stage LFD model.

Table 5 presents each pipe's average precision, recall, and F_1 score from 100 experiments. The average precision was 87.26%, and the average recall was 86.96%. The first-stage LFD model's precision and recall were above 85%. However, there were still some pipe categories with poor diagnosis results such as pipe numbers 1, 2, 3, 4, 7, 8, 15, and 16 in the case network (discussed in Section 4.1).

Table 5. First-stage LFD model's average performance metrics.

Pipe Number	Precision (*P*)	Recall (*R*)	F_1	Pipe Number	Precision (*P*)	Recall (*R*)	F_1
1	62.40%	66.53%	0.6440	16	66.07%	66.65%	0.6636
2	64.85%	66.18%	0.6551	17	92.39%	85.90%	0.8902
3	51.19%	51.55%	0.5137	18	95.58%	90.14%	0.9278
4	57.51%	60.86%	0.5914	19	96.08%	95.91%	0.9599
5	99.47%	98.19%	0.9882	20	93.68%	95.21%	0.9444
6	99.64%	97.90%	0.9876	21	99.06%	98.54%	0.9880

7	72.19%	73.08%	0.7263	22	99.52%	97.13%	0.9831
8	84.09%	84.98%	0.8453	23	99.11%	98.24%	0.9868
9	93.16%	91.86%	0.9251	24	97.60%	97.49%	0.9755
10	95.38%	92.93%	0.9414	25	97.85%	92.82%	0.9527
11	93.41%	92.10%	0.9251	26	96.50%	91.98%	0.9418
12	94.61%	95.67%	0.9514	27	92.54%	98.01%	0.9520
13	89.31%	89.67%	0.8949	28	89.66%	96.37%	0.9289
14	91.69%	91.80%	0.9174	29	98.44%	96.48%	0.9745
15	57.31%	60.13%	0.5869	30	97.47%	94.62%	0.9602

At the same time, in order to further evaluate the performance of the first-stage LFD model, two evaluation indicators—*accuracy* and *macro-F*$_1$—were selected to evaluate the overall performance of the model in 100 test sets. Figure 8 shows the accuracy and *macro-F*$_1$ of the BP-neural-network-based leak-stage diagnosis model for the ACWS network on the 100 test sets. The horizontal axis is the accuracy of the LFD model on the test set for each group of experiments, while the vertical axis is the macro-F1 of the LFD model on the test set.

As shown in Figure 8, the performance of the Adam-based LFD model was relatively stable in 100 sets of test experiments, and the classification *accuracy* of the LFD model for the case network was between 84.41% and 89.47%, while the *macro-F*$_1$ was between 0.8458 and 0.8966. After the final calculation, the average *accuracy* of the BP-neural-network-based LFD model was 86.96%, and its average *macro-F*$_1$ was 0.8709. The results show that the first-stage LFD model performs satisfactorily.

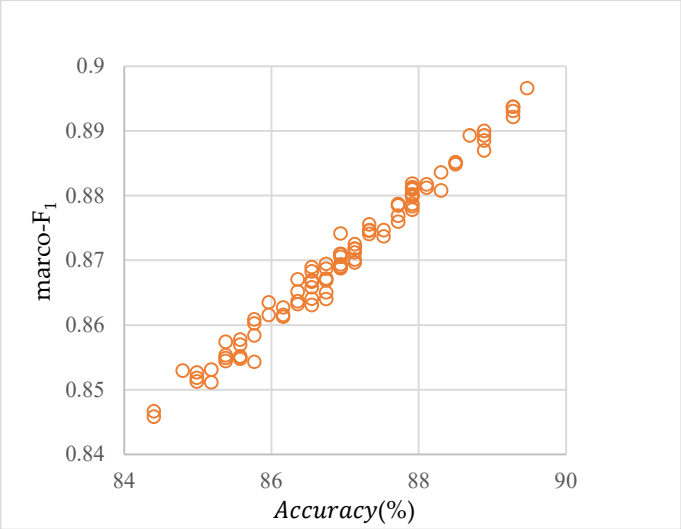

Figure 8. Performance metrics of the Adam-based LFD model on the test set.

3.3. Results of the Second-Stage LFD Model

In this case, a total of eight pipes exceeded the threshold of 50 m. According to the settings of the second-stage LFD model (detailed parameter settings are shown in Table 3), the Python programming language was also used for the training and testing of the neural network.

Figure 9 presents the average *MAE*, *MSE*, and R^2 values for each of the eight pipes under 100 test experiments, with a stable overall performance. The minimum *MSE* was 0.00518 and the maximum was 0.01117, with the average value being 0.00708, which is less than 0.01; the minimum R^2 value was 0.85 and the maximum was 0.93, with the average value being 0.90, which is greater than 0.9.

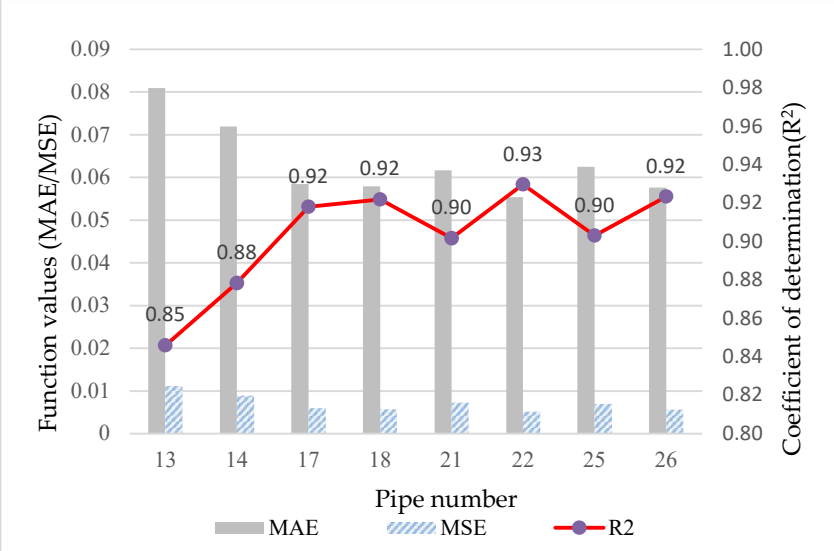

Figure 9. Second-stage LFD model performance in 100 sets of test experiments.

Taking the pipe13 leakage model as an example, the experimental results are presented for one randomly selected group out of 100 test experiments. Figure 10 shows the exact leakage locations and the model-predicted leakage locations in the test set. Except for a few outliers, the majority of the predicted values are close to the actual values, and it can be intuitively inferred that the BP-neural-network-based second-stage LFD model is able to predict the pipe leakage location accurately. Thus, the second-stage LFD model has good diagnostic efficacy.

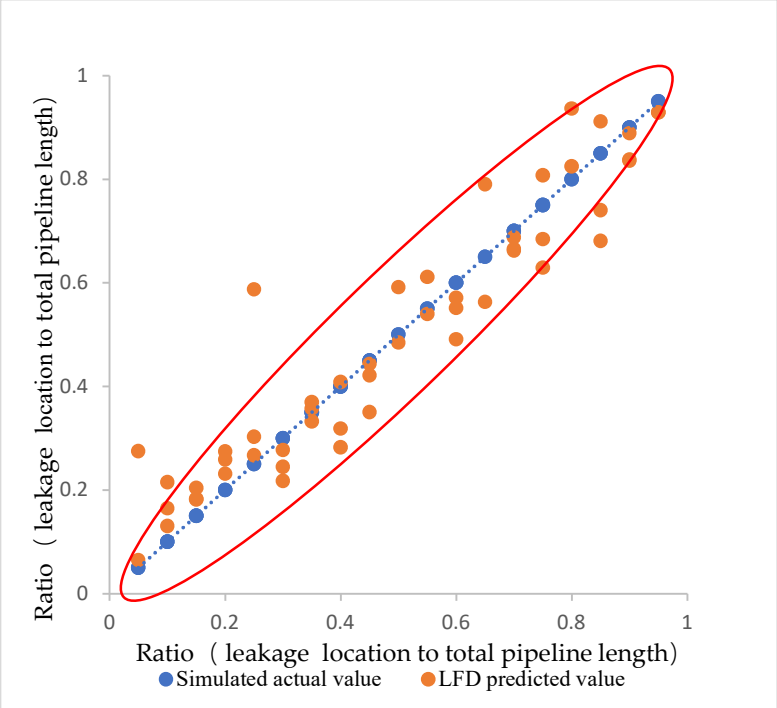

Figure 10. Distribution of simulated actual leakage locations and LFD-predicted locations for pipe13.

4. Discussions

4.1. Two-Stage LFD Model Discussion

The simulation results of the first-stage LFD model show that the diagnostic efficacy of some pipes is poor—such as pipe numbers 1, 2, 3, 4, 7, 8, 15, and 16—and the precision and recall rates are less than 85%. Therefore, the first-stage LFD model is prone to classification errors, resulting in incorrect diagnosis.

According to Table 4, the pipes with poor diagnostic efficacy of the first-level diagnosis model of pipe network leakage have the common characteristics of mutual connection and small resistance characteristic coefficients. Therefore, when these pipes have leakage failures, the parameter amplitude of the pipe network caused by leakage is limited—especially when the sensor reading itself has a certain random error—and the parameter change caused by the leakage of a pipe with a small resistance characteristic coefficient is easy to cover with noise, so it is difficult for the first-stage LFD model of the pipe network to achieve a diagnosis.

In response to the problem that the pipe network's LFD model is prone to misdiagnosis when leakage occurs in pipes with small resistance coefficients, this paper also seeks solutions from the following four perspectives:

(1) Improving the accuracy of sensors: Sensors with high accuracy should be installed and used as far as possible within the allowable range of conditions. The higher the accuracy level of the sensors, the less likely the reading error of the sensors to cover up the impact of pipe leakage, resulting in improved diagnostic accuracy of the LFD model.

(2) Cooperative diagnosis of multiple working conditions: In the event that it is difficult to make a diagnosis in a single working condition, the system's operating conditions can be switched to re-diagnose the leakage, and the fault diagnosis results of multiple working conditions can be used to collaboratively locate the leaky pipe section.

(3) Checking the second-ranking pipe based on probability distribution: Since the kernel of the LFD model is the probability distribution of the neural network algorithm, the second-ranking pipe in the probability ranking is checked, and if no fault occurs in this pipe, the pipes in the next ranking are checked by analogy.

(4) Combining pipe categories: Since the pipe categories prone to misclassification often have characteristics of low resistance and interconnection, it is useful to combine such pipes into one category and then carry out fault diagnosis, and when a fault is found in this category in practical application, all pipes within its combination should be inspected. Since the resistance characteristic coefficients of such pipes are small, and the pipe lengths are usually not too long, this does not theoretically increase the work difficulty of the maintenance personnel significantly.

In this case study, if pipes 1, 3, 7, and 15 and 2, 4, 8, and 16 are respectively combined into one category and other settings remain unchanged, the average accuracy of the BP-neural-network-based LFD model will be increased to 94.86%, which is 7.89% higher than the average accuracy before combining, It can be seen that the diagnostic effect of the first-stage LFD model can be improved by combining the pipe categories.

The simulation results of the second-stage LFD model show that the predicted value of the model is close to the simulated actual value under the leakage condition. The threshold set by the secondary leakage model in this paper is 50 m, and the average deviation between the predicted leakage point position and its actual position is 6.3% of the total length of the leaky pipe. This is acceptable for pipes over 50 m long. Applying the second-stage LFD model in engineering practice can help locate the exact leakage location of long pipes quickly, even if there are deviations, and when human initiative is exercised, maintenance workers can quickly locate the leakage point in the area near the resultant value, which plays an important role in reducing labor costs and improving time efficiency.

4.2. Limitations

In this paper, 11 flow sensors and 20 pressure sensors were installed in the ACWS network. The number of sensors in the case network is relatively complete, but in other projects, the number of sensors in many ACWSs is lower [27], which may reduce the performance of the LFD model, so the performance of the LFD model with different numbers of sensors should be explored in subsequent research.

At the same time, due to climate overheating [28], more passive design strategies are being added to buildings, which will lead to increased complexity and reduced reliability of air conditioning systems [29]. This directly affects the stability of ACWSs, so this factor should be considered in future research.

In addition, this paper is devoted to the study of pipeline leakage faults, which account for more than 80% of ACWS faults [30]. However, there are still blockage and junction problems in actual running water systems, which will be another direction for further research. Moreover, the ACWS pipe network leakage diagnosis method proposed in this paper only accounts for single-point pipe network leakage problems. Although the phenomenon of multiple simultaneous leakage failures is rare in the normal operation of running pipe network systems, there still exists a certain degree of possibility of this situation occurring. Therefore, the problem of multiple leakage faults occurring at the same time in ACWS pipe networks needs to be investigated in the future.

5. Conclusions

This paper proposes a leakage diagnosis method for ACWSs using an Adam optimization BP neural network algorithm, which is able to provide fault diagnosis. When a leak occurs in the actual pipe network system, the method locates the leaky pipe in the network and then locates the exact leakage location on the pipe. The main conclusions are summarized as follows:

(1) A hydraulic model that can simulate pipe network leakage was developed on the Dymola platform. In order to ensure the accuracy and reliability of the hydraulic model, a method of identifying the pipe network's resistance characteristics based on the cuckoo search algorithm was proposed, and the identification results of the algorithm were applied to the case of an ACWS pipe network. The average relative error of the flow rate at each terminal was 1.358%, the water supply pressure at each terminal was 0.057%, and the return water pressure at each terminal was 0.089%. The results show that the average relative error between the simulated values and the actual monitored values obtained using the method was no more than 1.5%. The hydraulic model was consistent with the real system, and it is practicable to generate the dataset under leakage conditions with this model.

(2) A two-stage LFD model based on the Adam-optimized BP neural network algorithm was proposed. The case study shows that the average accuracy of the first-stage LFD model for locating leaky pipes was 86.96%, and when the method of combining some pipe categories with smaller resistance characteristic coefficients was used, the average accuracy of the model increased to 94.86%. The second-stage LFD model of pipe network considers pipe's with a length of over 50 m in the ACWS system; the average R^2 of the second-stage LFD model was 0.9028, and the average error between the predicted location of the leakage point and its simulated actual location was 6.3% of the total length of the leakage pipe.

It should be noted that the hydraulic model of pipe network leakage built on the Dymola platform can be applied not only in ACWSs, but also in leakage studies of pipe networks of other engineering water systems (e.g., district heating pipe networks and municipal water supply networks). In addition, the proposed cuckoo search algorithm performs excellently in the identification of resistance characteristics of the pipe network, making the hydraulic model closer to the actual operating system, and providing a

method to achieve an accurate hydraulic model. Meanwhile, the proposed Adam-optimized BP neural network algorithm for the two-stage fault diagnosis model shows accuracy in practical engineering applications, providing a promising and sustainable solution for actual ACWS leakage problems. More importantly, the design concept of hierarchical diagnosis opens up the possibility of complex water system diagnosis, and the operation and maintenance of water systems will be more intelligent and efficient in the future.

Author Contributions: Conceptualization, R.L. and Y.Z.; data curation, R.L.; writing—original draft preparation, R.L.; writing—review and editing, R.L.; visualization, R.L.; methodology, R.L. and Y.Z.; software, Y.Z.; validation, R.L., Y.Z., and Z.L.; formal analysis, R.L. and Y.Z.; investigation, Y.Z.; resources, Z.L.; supervision, Z.L.; project administration, R.L.; funding acquisition, R.L. All authors have read and agreed to the published version of the manuscript.

Funding: This research received no external funding.

Institutional Review Board Statement: Not applicable.

Informed Consent Statement: Not applicable.

Data Availability Statement: Data is contained within the article.

Conflicts of Interest: The authors declare no conflict of interest.

Appendix A

The theoretical calculation method is the most commonly used method for hydraulic calculation of pipe networks under leakage conditions. Based on the constant flow condition of the pipe, the import and export pressure difference of the pipe under leakage conditions can be calculated using the Darcy formula.

Example: In a straight pipe with a total length of 10 m, the nominal diameter of the pipe is DN65, the absolute roughness of the inner wall of the pipe is 0.2 mm and the distribution is uniform, the water temperature in the pipe is 10 °C, the inlet flow of the pipe is always maintained at 10 L/s, and the flow rate of the fluid in the pipe is 3.0 m/s without leakage.

In order to avoid the influence of contingency on the results of a single experiment, a total of 10 different sets of experiments were set up. Each experiment was set up with a different leakage volume and leakage location (the leakage location was expressed as the ratio of the distance of the leakage point from the starting point of the pipe to the total pipe length). The experimental results are shown in Table A1.

Table A1. Pressure difference between the inlet and outlet of a pipe, as determined by two methods.

Number	Leakage Volume (L/s)	Leakage Location	Pressure Difference between the Inlet and Outlet of the Pipe (kP_a)		Relative Error (%)
			Theoretical Value	Simulated Value	
1	0	0	19.011	18.962	−0.257
2	0.1	0.1	18.675	18.627	−0.260
3	0.5	0.1	17.365	17.318	−0.273
4	1.0	0.1	15.802	15.757	−0.289
5	0.1	0.5	18.825	18.756	−0.365
6	0.5	0.5	18.097	18.049	−0.266
7	1.0	0.5	17.288	17.181	−0.273
8	0.1	0.9	18.974	18.925	−0.258
9	0.5	0.9	18.828	18.780	−0.259
10	1.0	0.9	18.655	18.606	−0.261

The results show that under different leakage conditions, the simulation results of the inlet and outlet pressure difference of the experimental pipe are very close to the theoretical calculation results. The maximum absolute value of the relative error is 0.365%, and the average error is −0.276. The error is usually within the acceptable range of hydraulic calculation, so the developed leakage hydraulic model is suitable for simulating the actual pipe leakage.

References

1. Wang, J.; Huang, J.; Fu, Q.; Gao, E.; Chen, J. Metabolism-based ventilation monitoring and control method for COVID-19 risk mitigation in gymnasiums and alike places. *Sustain. Cities Soc.* **2022**, *80*, 103719–103719.
2. Li, H.; Li, H.; Pei, H.; Li, Z. Leakage detection of HVAC pipeline network based on pressure signal diagnosis. *Build. Simul.* **2019**, *12*, 617–628.
3. Lu, Y. Practical Heating and Air Conditioning Design Manual. *Heat. Vent. Air Cond.* **2008**, *6*, 152.
4. Mulligan, S.; Hannon, L.; Ryan, P.; Nair, S.; Clifford, E. Development of a data driven FDD approach for building water networks: Water distribution system performance assessment rules. *J. Build. Eng.* **2021**, *34*, 101773.
5. Puust, R.; Kapelan, Z.; Savic, D.A.; Koppel, T. A review of methods for leakage management in pipe networks. *Urban Water J.* **2010**, *7*, 25–45.
6. Datta, S.; Sarkar, S. A review on different pipeline fault detection methods. *J. Loss Prev. Process Ind.* **2016**, *41*, 97–106.
7. Zhou, Z.; Zhang, J.; Huang, X.; Zhang, J.; Guo, X. Trend of soil temperature during pipeline leakage of high-pressure natural gas: Experimental and numerical study. *Measurement* **2020**, *153*, 107440.
8. Zhou, S.; O'neill, Z.; O'neill, C. A review of leakage detection methods for district heating networks. *Appl. Therm. Eng.* **2018**, *137*, 567–574.
9. Abdulshaheed, A.; Mustapha, F.; Ghavamian, A. A pressure-based method for monitoring leaks in a pipe distribution system: A Review. *Renew. Sustain. Energy Rev.* **2017**, *69*, 902–911.
10. Akkaya, A.E.; Talu, M.F. Extended kalman filter based IMU sensor fusion application for leakage position detection in water pipelines. *J. Fac. Eng. Archit. Gazi Univ.* **2017**, *32*, 1393–1404.
11. Abdulla, M.B.; Herzallah, R. Probabilistic multiple model neural network based leak detection system: Experimental study. *J. Loss Prev. Process Ind.* **2015**, *36*, 30–38.
12. Shen, Y.; Chen, J.; Fu, Q.; Wu, H.; Wang, Y.; Lu, Y. Detection of District Heating Pipe Network Leakage Fault Using UCB Arm Selection Method. *Buildings* **2021**, *11*, 275.
13. Zadkarami, M.; Shahbazian, M.; Salahshoor, K. Pipeline leakage detection and isolation: An integrated approach of statistical and wavelet feature extraction with multi-layer perceptron neural network (MLPNN). *J. Loss Prev. Process Ind.* **2016**, *43*, 479–487.
14. Lei, C.; Zhou, P. Application of neural network in heating network leakage fault diagnosis. *J. Southeast Univ. (Engl. Ed.)* **2010**, *26*, 173–176.
15. Duan, P.; Duan, L.; Tian, Q. ANFIS in Leakage Fault Diagnosis of Heating Networks. *J. Zhengzhou Univ. (Eng. Sci.)* **2014**, *35*, 56–60.
16. Xue, P.; Jiang, Y.; Zhou, Z.; Chen, X.; Fang, X.; Liu, J. Machine learning-based leakage fault detection for district heating networks. *Energy Build.* **2020**, *223*, 110161.
17. Banjara N K, Sasmal S, Voggu, S. Machine learning supported acoustic emission technique for leakage detection in pipelines. *Int. J. Press. Vessel. Pip.* **2020**, *188*, 104243.
18. Duan, H.F. Development of a TFR-Based Method for the Simultaneous Detection of Leakage and Partial Blockage in Water Supply Pipelines. *J. Hydraul. Eng.* **2020**, *146*, 04020051.
19. Hamza, G.; Hammadi, M.; Barkallah, M.; Choley, J.Y.; Riviere, A.; Louati, J.; Haddar, M. Compact Analytical Models for Vibration Analysis in Modelica/Dymola: Application to the Wind Turbine Drive Train System. *J. Chin. Soc. Mech. Eng.* **2018**, *39*, 121–130.
20. Civicioglu, P.; Besdok, E. A conceptual comparison of the Cuckoo-search, particle swarm optimization, differential evolution and artificial bee colony algorithms. *Artif. Intell. Rev.* **2013**, *39*, 315–346.
21. Iacca, G.; Dos Santos Junior, V.C.; De Melo, V.V. An improved Jaya optimization algorithm with Levy flight. *Expert Syst. Appl.* **2021**, *165*, 113902.
22. Yi, D.; Ahn, J.; Ji, S. An Effective Optimization Method for Machine Learning Based on ADAM. *Appl. Sci.* **2020**, *10*, 1073.
23. Fan, Q.; Guo, Y.; Wu, S.; Liu, X. Two-Level Diagnosis of Heating Pipe Network Leakage Based on Deep Belief Network. *IEEE Access* **2019**, *7*, 182983–182992.
24. Wen, L.; Li, X.Y.; Gao, L. A New Two-Level Hierarchical Diagnosis Network Based on Convolutional Neural Network. *IEEE Trans. Instrum. Meas.* **2020**, *69*, 330–338.
25. Fu, Q.; Li, K.; Chen, J.; Wang, J.; Lu, Y.; Wang, Y. Building Energy Consumption Prediction Using a Deep-Forest-Based DQN Method. *Buildings* **2022**, *12*, 131.
26. Qin, F.W.; Bai, J.; Yuan, W.Q. Research on intelligent fault diagnosis of mechanical equipment based on sparse deep neural networks. *J. Vibroeng.* **2017**, *19*, 2439–2455.

27. Wang, J.; Hou, J.; Chen, J.; Fu, Q.; Huang, G. Data mining approach for improving the optimal control of HVAC systems: An event-driven strategy. *J. Build. Eng.* **2021**, *39*, 102246.
28. Ozarisoy, B. Energy effectiveness of passive cooling design strategies to reduce the impact of long-term heatwaves on occupants' thermal comfort in Europe: Climate change and mitigation. *J. Clean. Prod.* **2022**, *330*, 129675.
29. Ozarisoy, B.; Altan, H. Regression forecasting of 'neutral' adaptive thermal comfort: A field study investigation in the south-eastern Mediterranean climate of Cyprus. *Build. Environ.* **2021**, *202*, 108013.
30. Sun, J.L.; Wang, R.H.; Duan, H.F. Multiple-fault detection in water pipelines using transient-based time-frequency analysis. *J. Hydroinform.* **2016**, *18*, 975–989.